arXiv:2009.00510v1 [hep-th] 1 Sep 2020

The instability of *AdS* black holes with lattices *

Yi Ling [1,2,3] Meng-He Wu [1,2]

[1] Institute of High Energy Physics, Chinese Academy of Sciences, Beijing, 100049, China
[2] School of Physics, University of Chinese Academy of Sciences, Beijing, 100049, China
[3] Shanghai Key Laboratory of High Temperature Superconductors, Shanghai,200444, China

Abstract: The Anti-de Sitter (AdS) black hole with lattice structure plays an essential role in the study of the optical conductivity in holographic approach. We investigate the instability of this sort of black holes which may lead to the holographic description of charge density waves. In the presence of homogeneous axion fields, we show that the instability of AdS-Reissner-Nordström(AdS-RN) black hole is always suppressed. However, in the presence of Q-lattices, we find that the unstable region becomes the smallest in the vicinity of the critical region for metal/insulator phase transition. This novel phenomenon is reminiscent of the behavior of the holographic entanglement entropy during quantum phase transition.

Key words: gauge/gravity duality, holographic gravity

PACS: 11.25.Tq, 04.70.bw

1 Introduction

In recent years the gauge/gravity duality has successfully been applied to the strongly coupled system in condense matter physics, which now as an important branch of holographic approach is dubbed as AdS/CMT duality [1]. It is well known that the instability of AdS black hole plays an essential role in order to achieve the abundant phase structure of the condensed matter system on the boundary. Especially, the spontaneous breaking of $U(1)$ gauge symmetry in the bulk leads to a new sort of black holes with scalar hair, which provides a novel picture for the condensation of superconductivity[2–4]. While the spontaneous breaking of translational invariance leads to the generation of spatially modulated modes for black holes, which is holographically dual to the formation of charge density waves (CDW)[5–16]. For high T_c superconductor, the charge density wave phase is also named as the pseudo-gap phase, which plays a key role in understanding the formation of high T_c superconductivity[17].

Originally the holographic CDW is formed over an AdS-RN background with translational symmetry. The basic idea is to introduce unstable terms into the action such that the BF bound of AdS black holes is violated below some value of the Hawking temperature. As a result, the ordinary AdS-RN background becomes unstable and flows to a new configuration which exhibits a periodic structure along a spatial direction, giving rise to the formation of CDW. In this paper we intend to investigate the instability of a sort of AdS-RN black holes *without* translational invariance. In AdS/CMT duality, it is essential to construct a bulk geometry without translational invariance in order to obtain a finite direct current (DC) conductivity for the dual system. If the translational symmetry is preserved, then the momentum would be conserved such that the DC would flow without relaxation, giving rise to an infinite conductivity. This of course is not the feature of practical materials. Now in holographic framework, typically one has two ways to break the translational symmetry by hand (for brief review see [18]). One way is to construct a lattice manifestly by introducing spatially modulated sources in the bulk [19–23]. However, in this framework it is very challenging to explore the low temperature effects due to the numerical difficulties involved in solving partial differential equations (PDEs) [24]. An alternative way is to introduce the momentum dissipation by linear axion fields, helical lattice or Q-lattices, which might be called as "homogeneous lattices"[25–37]. In these models, though the translation symmetry is broken, the equations of motion are still ordinary differential equations (ODEs) which can be numerically solved even in the zero temperature limit. Remarkably, in this framework a novel metal/insulator transition has been observed[25], which makes it plausible to study the quantum critical phenomenon in the holographic setup with lattices[31].

∗ We are very grateful to Peng Liu, Yuxuan Liu, Chao Niu, Jianpin Wu and Zhuoyu Xian for helpful discussions and former collaborations on building holographic lattices. This work is supported by the Natural Science Foundation of China under Grant No. 11875053.

1) E-mail: lingy@ihep.ac.cn
2) E-mail: mhwu@ihep.ac.cn

Therefore, it is very desirable to construct holographic CDW over a lattice background rather than a background with translational symmetry. This is the main motivation of this paper. As the first step, we will investigate the instability of a sort of AdS black holes with homogeneous lattices by perturbative analysis. We will determine the unstable region in the configuration space in the presence of axion fields and Q-lattices, respectively. We will demonstrate that the presence of the linear axion field always suppresses the instability of AdS-RN black hole. However, in Q-lattice framework, we find that in low temperature limit, the unstable region becomes the smallest near the critical region of the metal/insulator transition. This novel phenomenon is reminiscent of the role of holographic entanglement entropy, which signals the occurrence of quantum phase transition.

This paper is organized as follows. In Section 2 , we introduce the holographic model for charge density waves, and briefly review the instability of the AdS-RN black hole. In Section 3, we analyze the instability of the black hole with momentum relaxation due to the linear axion fields. Then we focus on the instability of the Q-lattice background in Section 4. Our results and conclusions are given in Section 5.

2 The holographic setup

In this section, we introduce a holographic model without lattice structure in four dimensional spacetime, in which the gravity is coupled to a dilaton field and two massless $U(1)$ gauge fields. Then in next sections we will impose lattice structure based on this setup. The action is given by,

$$S=\frac{1}{2\kappa^2}\int d^4x\sqrt{-g}\ \mathfrak{L}_1, \tag{1}$$

where

$$\mathfrak{L}_1= \quad R-\frac{1}{2}\left(\nabla\Phi\right)^2-V\left(\Phi\right)-\frac{1}{4}Z_A(\Phi)F^2-\frac{1}{4}Z_B(\Phi)G^2-\frac{1}{2}Z_{AB}(\Phi)FG, \tag{2}$$

with $F=dA$, $G=dB$. Two gauge fields A and B correspond to two global $U(1)$ symmetries on the boundary. We will treat gauge field B as the electromagnetic field and consider its transport properties. The real dilaton field Φ will be viewed as the order parameter of translational symmetry breaking. We propose that functions V, Z_A, Z_B, Z_{AB} have the following form:

$$\begin{aligned} V(\Phi)&=-\frac{1}{L^2}+\frac{1}{2}m_s^2\Phi^2,\\ Z_A(\Phi)&=1-\frac{\beta}{2}L^2\Phi^2,\\ Z_B(\Phi)&=1,\\ Z_{AB}(\Phi)&=\frac{\gamma}{\sqrt{2}}L\Phi. \end{aligned} \tag{3}$$

In above setup two important terms are introduced. One is the β-term, which plays an essential role in inducing the instability of AdS-RN black holes to form CDW, while the other γ-term is not essential, just driving the tip of the unstable dome deviating from $k_c=0$.

The equations of motion are given by

$$\begin{aligned} &R_{\mu\nu}-T^{\Phi}_{\mu\nu}-T^{A}_{\mu\nu}-T^{B}_{\mu\nu}-T^{AB}_{\mu\nu}=0,\\ &\nabla^2\Phi-\frac{1}{4}Z'_AF^2-\frac{1}{4}Z'_BG^2-V'=0,\\ &\nabla_\mu(Z_AF^{\mu\nu}+Z_{AB}G^{\mu\nu})=0,\\ &\nabla_\mu(Z_BG^{\mu\nu}+Z_{AB}F^{\mu\nu})=0, \end{aligned} \tag{4}$$

where

$$\begin{aligned} T^{\Phi}_{\mu\nu}&=\frac{1}{2}\nabla_\mu\Phi\nabla_\nu\Phi+\frac{1}{2}Vg_{\mu\nu},\\ T^{A}_{\mu\nu}&=\frac{Z_A}{2}\left(F_{\mu\rho}F^{\rho}_{\nu}-\frac{1}{4}g_{\mu\nu}F^2\right),\\ T^{B}_{\mu\nu}&=\frac{Z_B}{2}\left(G_{\mu\rho}G^{\rho}_{\nu}-\frac{1}{4}g_{\mu\nu}G^2\right),\\ T^{AB}_{\mu\nu}&=Z_{AB}\left(G_{(\mu|\rho|}F^{\rho}_{\nu)}-\frac{1}{4}g_{\mu\nu}GF\right). \end{aligned} \tag{5}$$

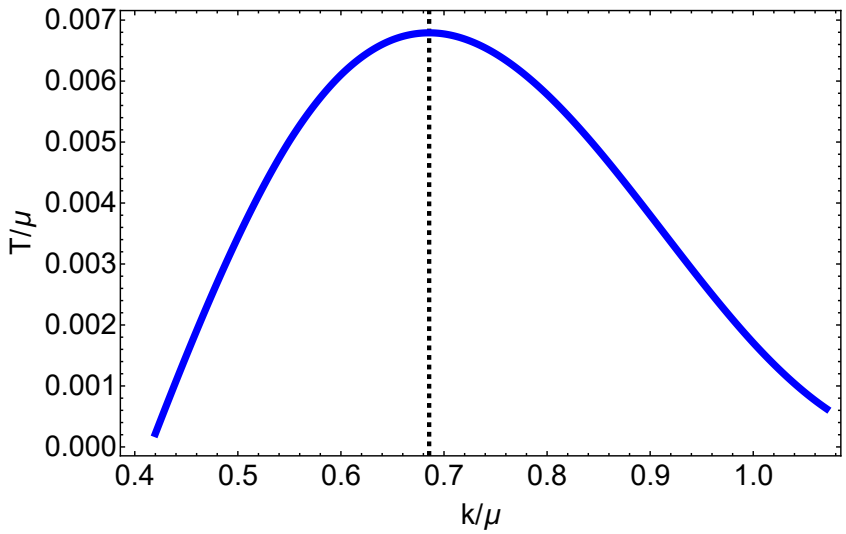


Fig. 1. The critical temperature as the function of the wave number. Below the curve is the unstable region which looks like a dome. The dashed line marks the location of the tip of the dome, with $k_c \approx 0.6856$.

The equations of motion admit the planar AdS-RN black hole as a solution with translational symmetry along both x and y directions, which is given as

$$\begin{aligned} ds^2 &= \frac{1}{z^2}\left[-(1-z)p(z)dt^2 + \frac{dz^2}{(1-z)p(z)} + dx^2 + dy^2\right], \\ A_t &= \mu(1-z),\ \Phi = 0,\ B = 0, \end{aligned} \tag{6}$$

where $p(z) = 4\left(1+z+z^2-\frac{\mu^2 z^3}{16}\right)$, μ is the chemical potential of gauge field A. In this coordinate system, the black hole horizon is located at $z=1$ and the AdS boundary is at $z=0$. The Hawking temperature of the black hole is simply given by $T/\mu = (48-\mu^2)/(16\pi\mu)$. Throughout this paper we shall set the AdS radius $l^2 = 6L^2 = 1/4$. Without loss of generality, two coupling constants will be set as $\beta = -94$ and $\gamma = 16.4$.

We remark that to analyze the instability of AdS black holes, the key point is that in zero temperature limit, the near horizon geometry of AdS-RN black holes is $AdS_2 \times R^2$. Once the BF bound of AdS_2 is violated, the near horizon geometry will become unstable and flow to a new solution as the infrared fixed point, which is characterized by the appearance of the spatially modulated modes in the bulk. And such analogous instability remains at finite temperature for AdS-RN black holes (for details we refer to [5]). Now specifically, we consider the following perturbations to examine the instability of the electrically charged AdS-RN black hole,

$$\begin{aligned} \delta\Phi &= \phi(z)\cos(kx), \\ \delta B &= b_t(z)\cos(kx). \end{aligned} \tag{7}$$

The instability of the background will be signaled by the existence of non-trivial solutions to the perturbation equations of $\delta\Phi$ and δB, which spontaneously break the translational symmetry along x direction. Taking the AdS-RN as the background and substituting (7) into the equations of motion (4), we obtain two coupled linear differential equations for $\phi(z)$ and $b_t(z)$. We impose the regular boundary condition at the horizon $z=1$. While near the AdS boundary $z=0$, we can expand $\phi(z)$ and $b_t(z)$ as

$$\begin{aligned} \phi(z) &\approx \phi_s z^{3-\Delta_\phi} + \phi_o z^{\Delta_\phi} + \cdots, \\ b_t(z) &\approx b_s z^{2-\Delta_B} + b_o z^{\Delta_B - 1} + \cdots, \end{aligned} \tag{8}$$

where $\Delta_\phi = 3/2 + \sqrt{9/4 + m_s^2 l^2}$ and $\Delta_B = 2$. We turn off the source terms, namely $\phi_s = b_s = 0$. Whether there exist non-trivial solutions to these equations depends on the wave number k as well as the Hawking temperature of black hole background. For illustration, we take the mass of the dilaton $m_s^2 = -2/l^2 = -8$. In Fig. 1, we plot the critical temperature as the function of wave number. It is clearly seen that the curve exhibits the bell curve behavior and the unstable region looks like a dome. The highest critical temperature is $T_{max}/\mu \approx 0.0068$, with wave number

$k_c/\mu \approx 0.6856$. Within the dome, the AdS-RN black hole becomes unstable and the charge density of gauge field B becomes spatially modulated.

3 The instability of black holes with axion fields

In this section, we consider the instability of black holes without translational invariance by adding axion fields into the above action, which becomes

$$S = \frac{1}{2\kappa^2}\int d^4x\sqrt{-g}\ (\mathfrak{L}_1 + \mathfrak{L}_{axions}), \tag{9}$$

with $\mathfrak{L}_1$ is given by (2), and

$$\mathfrak{L}_{axions} = \ -\frac{1}{2}\sum_{a=1}^{2}(\nabla\chi_a), \tag{10}$$

where χ_a are two real, massless scalar fields. This model allows a very simple but exact solution with momentum relaxation, which is given as

$$\begin{aligned} ds^2 &= \frac{1}{z^2}\left[-(1-z)U(z)dt^2 + \frac{dz^2}{(1-z)U(z)} + dx^2 + dy^2\right], \\ A_t &= \mu(1-z), \chi_1 = \alpha x\ , \chi_2 = \alpha y\ , \Phi = 0,\ B = 0, \end{aligned} \tag{11}$$

where $U(z) = 4+4z-\frac{1}{2}(\alpha^2-8)z^2-\frac{1}{4}\mu^2 z^3$. The presence of the axion fields will introduce momentum relaxation in both x and y directions, leading to a finite DC conductivity[27]. Here we are concerned with its impact on the instability of the background. Without loss of generality, we consider the perturbations with spatially modulated modes in x direction. In the left of Fig.2, we plot the critical temperature versus the wave number k/μ and the amplitude of axion fields α/μ. It is obvious that with the increase of the amplitude α/μ, the unstable region becomes smaller, indicating that the instability of the black hole is suppressed by the presence of the axion field. We also plot the highest critical temperature T_{max}/μ and the corresponding wave number k_c/μ as a function of α/μ, as illustrated in the middle and right of Fig.2. We notice that k_c/μ grows linearly with large α/μ, while T_{max}/μ drops down quickly with α/μ. This phenomenon is similar to what observed in other holographic models[39].

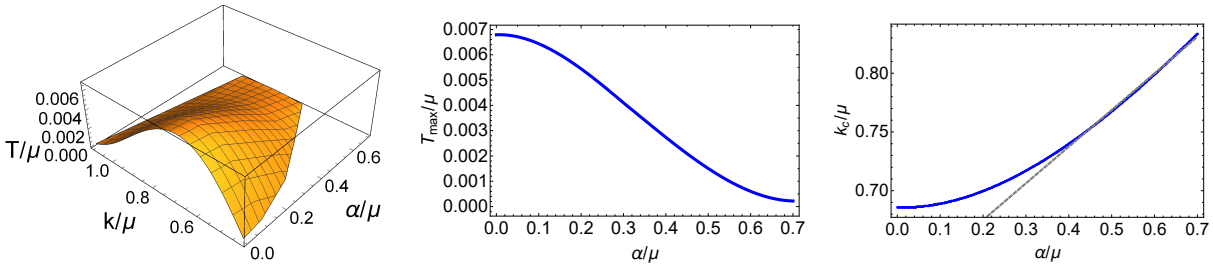


Fig. 2. The left 3D plot is the critical temperature versus the wave number k/μ and the amplitude of the axion field α/μ. The middle plot is the highest critical temperature T_{max}/μ versus the amplitude of the axion field α/μ. The right plot is the wave number k_c versus the amplitude of the axion field α/μ.

4 The instability of black holes with Q-lattice

In this section we consider the instability of black holes with Q-lattice[26]. Now the action becomes

$$S = \frac{1}{2\kappa^2}\int d^4x\sqrt{-g}\ (\mathfrak{L}_1 + \mathfrak{L}_Q), \tag{12}$$

with $\mathfrak{L}_1$ in (2) and

$$\mathfrak{L}_Q = \ -(|\nabla\Psi|^2 + m_q|\Psi|^2), \tag{13}$$

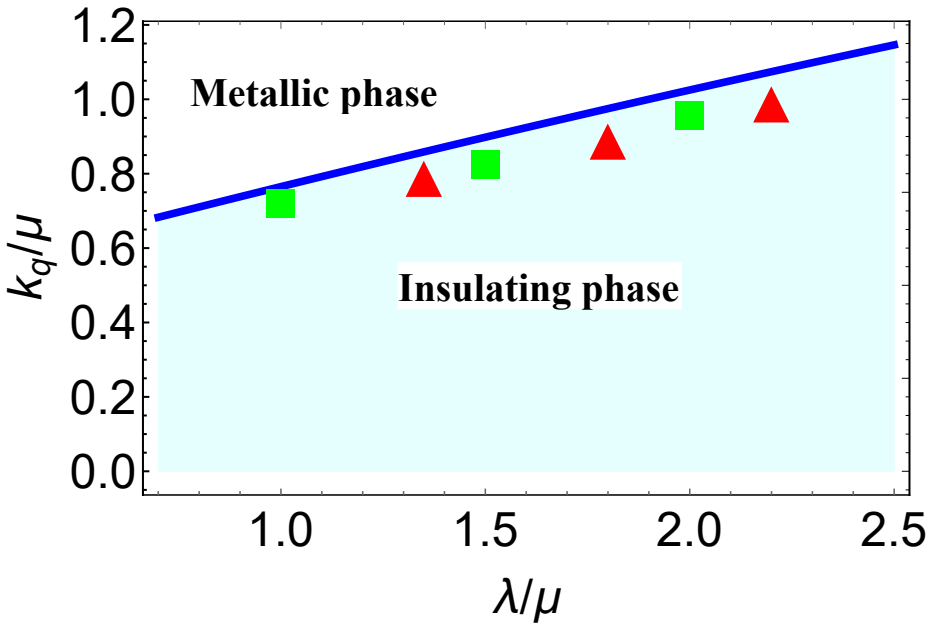


Fig. 3. The phase diagram for Q-lattice system at temperature $T/\mu = 0.001$. The red triangles stand for the valleys of the highest critical temperatures T_{max}/μ when varying λ/μ but fixing k_q/μ. The green squares stand for the valleys of the highest critical temperatures T_{max}/μ when varying k_q/μ but fixing λ/μ.

where Ψ is a complex scalar field. Then the Einstein equations become

$$R_{\mu\nu} - T^{\Phi}_{\mu\nu} - T^{A}_{\mu\nu} - T^{B}_{\mu\nu} - T^{AB}_{\mu\nu} - T^{\Psi}_{\mu\nu} = 0, \tag{14}$$

with $T^{\Phi}_{\mu\nu}$ $T^{A}_{\mu\nu}$, $T^{B}_{\mu\nu}$, $T^{AB}_{\mu\nu}$ in (4) and

$$T^{\Psi}_{\mu\nu} = \nabla_{\mu}\Psi\nabla_{\nu}\Psi^{*} + \frac{1}{2}m_q^2|\Psi|^2 g_{\mu\nu}. \tag{15}$$

In addition, we have an equation of motion for Ψ,

$$(\nabla^2 - m_q)\Psi = 0. \tag{16}$$

We consider the following ansatz for the electrically charged AdS-RN black hole on Q-lattice,

$$\begin{aligned} ds^2 &= \frac{1}{z^2}\left[-(1-z)p(z)Udt^2 + \frac{dz^2}{(1-z)p(z)U} + V_1 dx^2 + V_2 dy^2\right], \\ A_t &= \mu(1-z)a, \Psi = e^{ik_q x} z^{3-\Delta_q}\psi,\ \Phi = 0,\ B = 0, \end{aligned} \tag{17}$$

with $\Delta_q = 3/2 \pm (9/4 + m_q^2 l^2)$. We choose the mass of scalar field to be $m_q^2 = -8$. Note that U, V_1, V_2, ψ and a are function of the radial coordinate z only. If one sets $U = V_1 = V_2 = a = 1$ and $\psi = 0$, then it goes back to the standard AdS-RN black hole. For the non-trivial Q-lattice solution, the boundary conditions at $z = 0$ are given by

$$U = V_1 = V_2 = a = 1,\ \psi = \lambda,\ \Phi = 0,\ B = 0, \tag{18}$$

and we take regular boundary condition on the horizon. As a result, a typical black hole solution with Q-lattice is characterized by three scale invariant parameters which are T/μ, λ/μ and k_q/μ.

One remarkable feature of these Q-lattice background is that they exhibit a novel metal/insulatore transition when we adjust the lattice parameters λ/μ and k_q/μ in low temperature limit[25], and the phase diagram for metal/insulator phases over Q-lattice background has been studied in Ref.[28, 31]. For a given background, the DC conductivity can be expressed in terms of the horizon data as

$$\sigma_{DC} = \left(\sqrt{\frac{V_2}{V_1}} + \frac{\mu^2 a^2 \sqrt{V_1 V_2}}{k_q^2 \psi^2}\right)\Big|_{z=1}. \tag{19}$$

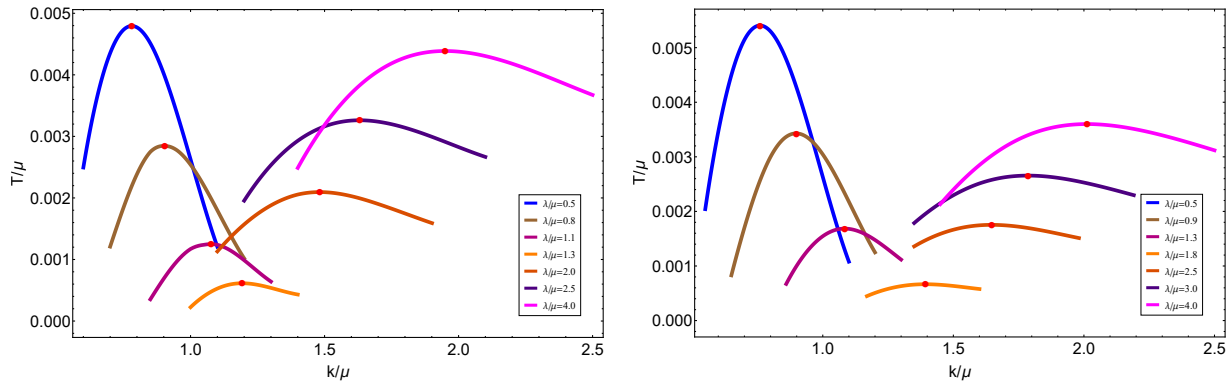


Fig. 4. The unstable region of the background with different values of λ/μ when the wave number of Q-lattice k_q is fixed as $k_q/\mu = 0.8$(left) and $k_q/\mu = 0.9$(right). The red dots mark the highest critical temperature on each curve with the corresponding wave number k_c/μ.

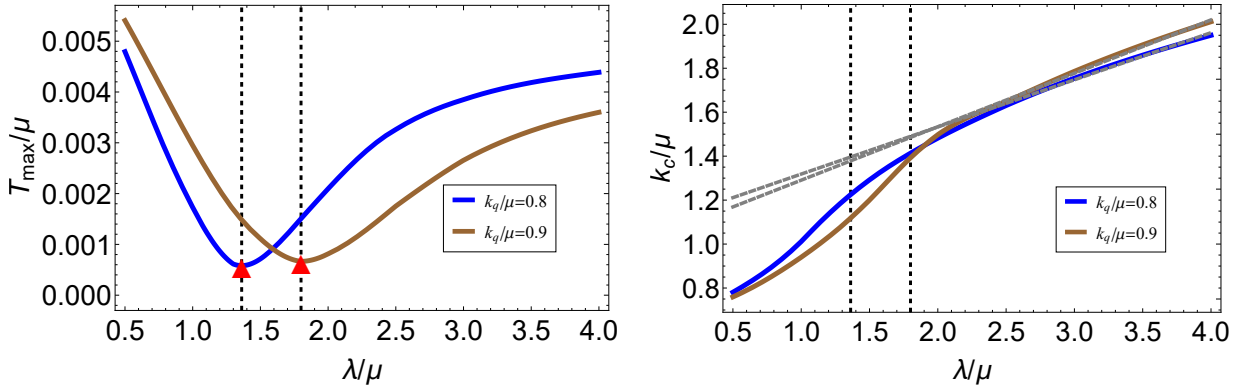


Fig. 5. The highest critical temperature T_{max}/μ and the wave number k_c/μ as the function of the lattice amplitude λ/μ for the given wave number $k_q/\mu = 0.8$ and $k_q/\mu = 0.9$.

Throughout this paper we identify the metallic phase and the insulating phase by evaluating Eq.(19) around $T/\mu = 0.001$. The quantum critical line is given by $\partial_T \sigma_{DC} = 0$. In Fig. 3, we demonstrate the phase diagram for Q-lattice system.

Now we focus on the instability of this sort of black holes with lattices. In Fig. 4, we plot the unstable region of the background with different values of λ/μ when the wave number of Q-lattice k_q/μ is fixed as $k_q/\mu = 0.8$ and $k_q/\mu = 0.9$, respectively. The region below each curve is the unstable region where the spatially modulated modes with wave number k/μ may emerge. In contrast to the results observed in axion model in previous section, we find the unstable region does not change monotonously with the lattice parameter any more. To our surprise, we find the unstable region becomes smaller with the increase of λ/μ at first, but later it becomes larger again. To disclose this with more transparency, we may mark the highest critical temperature T_{max}/μ with red dot on each curve and denote the corresponding wave number as k_c/μ. Then we plot T_{max}/μ and k_c/μ as the function of the lattice amplitude λ/μ, as illustrated in Fig. 5. It is obvious to see that T_{max}/μ reaches the minimal value and then rises up again with the increase of λ/μ. Going back to the phase diagram of the Q-lattice, we find the turning points are quite close to the critical line for metal/insulator transition! To check this we may also plot the unstable region of the background with different values of k_q/μ but fixing the lattice amplitude λ/μ, as illustrated in Fig.6. Correspondingly, T_{max}/μ and k_c/μ as the function of the wave number k_q/μ is plotted in Fig.7. Again, we find that the turning points of T_{max}/μ are quite close to the critical line, as marked in Fig.3. Since the curve with the minimal value of T_{max}/μ encloses the smallest region of instability, as illustrated in Fig. 4, we conclude that the black hole background in the vicinity of metal/insulator transition is the most stable solutions under the perturbations of spatial modulated modes given by (8).

First of all, it is quite interesting to compare the change of T_{max}/μ of CDW with that of superconductivity with the change of Q-lattice parameters, which was previously investigated in [28]. It is found that the critical temperature of superconductivity is always suppressed by the presence of the Q-lattice. When the lattice effect is strong enough,

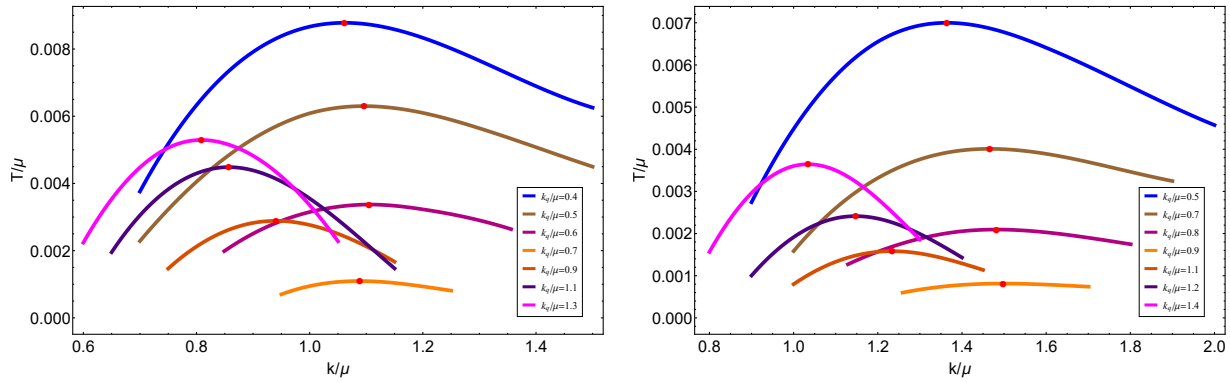


Fig. 6. The unstable region of the background with different values of k_q/μ when the lattice amplitude λ/μ is fixed as $\lambda/\mu = 1$(left) and $\lambda/\mu = 2$(right). The red dots mark the highest critical temperature on each curve with the corresponding wave number k_c/μ.

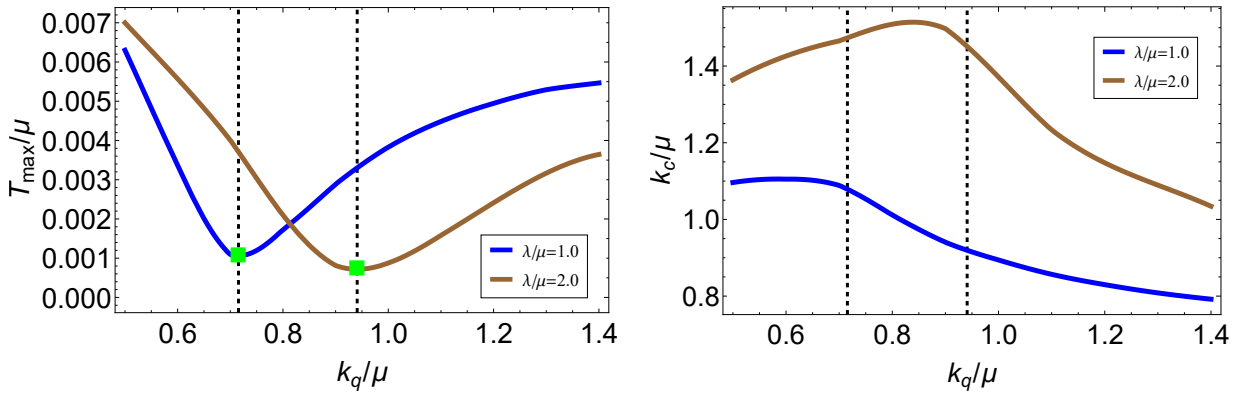


Fig. 7. The highest critical temperature T_{max}/μ and the wave number k_c/μ as the function of the lattice wave number k_q/μ for the given amplitude $\lambda/\mu = 1$ and $\lambda/\mu = 2$.

the critical temperature of superconductivity drops down to zero such that the superconducting phase disappears. However, for CDW the critical temperature will rise up again with the increase of lattice parameters, which means the background becomes more unstable and it is easier to form a new background with CDWs. This difference may be understood based on the phase diagram of Q-lattice background as demonstrated in Fig.3. For large λ/μ, the dual system falls into a deep insulating phase. Therefore, it is quite nature to understand that it becomes harder to form superconductivity over such insulating phases. On the contrary, the CDW phase itself is an insulating phase. Thus such a background dual to a deep insulating phase will assist the formation of CDW.

This phenomenon indicates that the instability of the background might be used to characterize the occurrence of quantum phase transition. It is well known that in the absence of ordinary order parameters, it is very hard to diagnose quantum phase transitions. Previously the role of holographic entanglement entropy in diagnosing the quantum phase transition has been disclosed in a series of papers[31, 33, 38]. The holographic entanglement entropy or its derivative with respect to system parameters displays a peak or valley in the vicinity of the critical region. Here we find T_{max}/μ of CDW exhibits a similar behavior as the entanglement entropy. Physically, it implies that the system becomes rather stable under the perturbations with spatially modulated modes near the critical point of quantum phase transition in zero temperature limit. Intuitively, this might be understood as follows. The formation of CDW over a fixed background results from a thermodynamical phase transition. Near the critical point of quantum phase transition, the system becomes long-range correlated such that the effects of thermal perturbations would be suppressed, leading to a more stable background with the lowest T_{max}/μ.

Finally, we may also give a comment on the commensurability of this sort of black holes with lattice, which involves in the comparison between the wave number of CDW, namely k_c/μ and the wave number of lattices. We plot k_c/μ as the function of the lattice amplitude λ/μ in Fig. 5 and the wave number of Q-lattice k_q/μ in Fig. 7, respectively. We find that k_c/μ grows linearly with the amplitude of Q-lattice λ/μ for large λ/μ. However, it decreases with the wave number of Q-lattice k_q/μ for large k_q/μ. No manifest effect or phenomenon is observed when

$k_c/\mu = k_q/\mu$. The commensurability seems absent in this setup, similar to the result observed in [39].

5 Discussion

In this paper we have investigated the instability of black holes with momentum relaxation. It is found that the presence of linear axion fields suppresses the instability of AdS-RN black hole. The wave number k_c/μ of spatially modulated modes grows linearly with the axion field α/μ for large α/μ. More importantly, in Q-lattice framework we have demonstrated that in zero temperature limit the unstable dome is the smallest near the critical region of metal/insulator transition. The highest critical temperature T_{max}/μ displays a valley near the critical points of metal/insulator transition. This novel phenomenon is reminiscent of the behavior of the holographic entanglement entropy during quantum phase transition. We conjecture that any instability of background leading to a thermodynamical phase transition would be greatly suppressed in the critical region of quantum phase transition, since in this region the system becomes long-range correlated. The commensurate effect is absent in both models with homogeneous lattices, similar to the results obtained in Ref.[39].

In this paper we have only presented the perturbation analysis over a fixed background to justify the instability of this background. To explicitly construct a new background with both lattices and CDW, one needs to go beyond the perturbation analysis and solve all the equations of motion numerically, which are PDEs rather than ODEs. It is completely plausible to obtain such solutions at normal temperatures, as investigated in [5, 6]. However, as we mentioned in the introduction, finding numerical solutions would become rather difficult in zero temperature limit. Our analysis on the instability of black holes in this paper sheds light on the construction of CDW background with Q-lattice in zero temperature limit since the critical temperature and the unstable region have been manifestly disclosed at extremely low temperature.

The phase diagram for high T_c superconductivity exhibits a very abundant structure with many universal features. Currently it is still challenging to exactly duplicate this phase diagram in holographic approach. Based on our current work, one may further introduce the complex scalar field as the order parameter of superconductivity, and consider the condensation of superconductivity due to $U(1)$ gauge symmetry breaking. Then it would be quite interesting to investigate the relations between CDW and superconductivity over such a lattice background.

References

1 S. A. Hartnoll, A. Lucas and S. Sachdev, [arXiv:1612.07324 [hep-th]].
2 S. S. Gubser, Phys. Rev. D **78**, 065034 (2008) doi:10.1103/PhysRevD.78.065034 [arXiv:0801.2977 [hep-th]].
3 S. A. Hartnoll, C. P. Herzog and G. T. Horowitz, Phys. Rev. Lett. **101**, 031601 (2008) doi:10.1103/PhysRevLett.101.031601 [arXiv:0803.3295 [hep-th]].
4 S. A. Hartnoll, C. P. Herzog and G. T. Horowitz, JHEP **12**, 015 (2008) doi:10.1088/1126-6708/2008/12/015 [arXiv:0810.1563 [hep-th]].
5 A. Donos and J. P. Gauntlett, Phys. Rev. D **87**, no.12, 126008 (2013) doi:10.1103/PhysRevD.87.126008 [arXiv:1303.4398 [hep-th]].
6 Y. Ling, C. Niu, J. Wu, Z. Xian and H. b. Zhang, Phys. Rev. Lett. **113**, 091602 (2014) doi:10.1103/PhysRevLett.113.091602 [arXiv:1404.0777 [hep-th]].
7 N. Jokela, M. Jarvinen and M. Lippert, JHEP **12**, 083 (2014) doi:10.1007/JHEP12(2014)083 [arXiv:1408.1397 [hep-th]].
8 E. Kiritsis and L. Li, JHEP **01**, 147 (2016) doi:10.1007/JHEP01(2016)147 [arXiv:1510.00020 [cond-mat.str-el]].
9 S. Cremonini, L. Li and J. Ren, Phys. Rev. D **95**, no.4, 041901 (2017) doi:10.1103/PhysRevD.95.041901 [arXiv:1612.04385 [hep-th]].
10 T. Andrade and A. Krikun, JHEP **03**, 168 (2017) doi:10.1007/JHEP03(2017)168 [arXiv:1701.04625 [hep-th]].
11 S. Cremonini, L. Li and J. Ren, JHEP **08**, 081 (2017) doi:10.1007/JHEP08(2017)081 [arXiv:1705.05390 [hep-th]].
12 N. Jokela, M. Jarvinen and M. Lippert, Phys. Rev. D **96**, no.10, 106017 (2017) doi:10.1103/PhysRevD.96.106017 [arXiv:1708.07837 [hep-th]].
13 S. Cremonini, L. Li and J. Ren, JHEP **12**, 080 (2018) doi:10.1007/JHEP12(2018)080 [arXiv:1807.11730 [hep-th]].
14 G. Song, Y. Seo and S. J. Sin, Int. J. Mod. Phys. A **35**, no.22, 2050128 (2020) doi:10.1142/S0217751X20501286 [arXiv:1810.03312 [hep-th]].
15 S. Cremonini, L. Li and J. Ren, JHEP **09**, 014 (2019) doi:10.1007/JHEP09(2019)014 [arXiv:1906.02753 [hep-th]].
16 A. Amoretti, D. Aren, B. Goutraux and D. Musso, JHEP **01**, 058 (2020) doi:10.1007/JHEP01(2020)058 [arXiv:1910.11330 [hep-th]].
17 Y. Ling, P. Liu and M. H. Wu, arXiv:1911.10368 [hep-th].
18 Y. Ling, Int. J. Mod. Phys. A **30**, no. 28,29, 1545013 (2015). doi:10.1142/S0217751X1545013X
19 G. T. Horowitz, J. E. Santos and D. Tong, JHEP **07**, 168 (2012) doi:10.1007/JHEP07(2012)168 [arXiv:1204.0519 [hep-th]].
20 G. T. Horowitz, J. E. Santos and D. Tong, JHEP **11**, 102 (2012) doi:10.1007/JHEP11(2012)102 [arXiv:1209.1098 [hep-th]].
21 G. T. Horowitz and J. E. Santos, JHEP **06**, 087 (2013) doi:10.1007/JHEP06(2013)087 [arXiv:1302.6586 [hep-th]].
22 Y. Ling, C. Niu, J. P. Wu, Z. Y. Xian and H. b. Zhang, JHEP **07**, 045 (2013) doi:10.1007/JHEP07(2013)045 [arXiv:1304.2128 [hep-th]].
23 Y. Ling, C. Niu, J. P. Wu and Z. Y. Xian, JHEP **11**, 006 (2013) doi:10.1007/JHEP11(2013)006 [arXiv:1309.4580 [hep-th]].
24 S. A. Hartnoll and J. E. Santos, Phys. Rev. D **89**, no.12, 126002 (2014) doi:10.1103/PhysRevD.89.126002 [arXiv:1403.4612 [hep-th]].
25 A. Donos and S. A. Hartnoll, Nature Phys. **9**, 649 (2013) doi:10.1038/nphys2701 [arXiv:1212.2998 [hep-th]].
26 A. Donos and J. P. Gauntlett, JHEP **04**, 040 (2014) doi:10.1007/JHEP04(2014)040 [arXiv:1311.3292 [hep-th]].
27 T. Andrade and B. Withers, JHEP **05**, 101 (2014) doi:10.1007/JHEP05(2014)101 [arXiv:1311.5157 [hep-th]].

28 Y. Ling, P. Liu, C. Niu, J. P. Wu and Z. Y. Xian, JHEP **02**, 059 (2015) doi:10.1007/JHEP02(2015)059 [arXiv:1410.6761 [hep-th]].
29 M. Baggioli and O. Pujolas, Phys. Rev. Lett. **114**, no.25, 251602 (2015) doi:10.1103/PhysRevLett.114.251602 [arXiv:1411.1003 [hep-th]].
30 R. A. Davison and B. Goutraux, JHEP **01**, 039 (2015) doi:10.1007/JHEP01(2015)039 [arXiv:1411.1062 [hep-th]].
31 Y. Ling, P. Liu, C. Niu, J. P. Wu and Z. Y. Xian, JHEP **04**, 114 (2016) doi:10.1007/JHEP04(2016)114 [arXiv:1502.03661 [hep-th]].
32 B. Goutraux, E. Kiritsis and W. J. Li, JHEP **04**, 122 (2016) doi:10.1007/JHEP04(2016)122 [arXiv:1602.01067 [hep-th]].
33 Y. Ling, P. Liu and J. P. Wu, Phys. Rev. D **93**, no.12, 126004 (2016) doi:10.1103/PhysRevD.93.126004 [arXiv:1604.04857 [hep-th]].
34 T. Andrade, M. Baggioli, A. Krikun and N. Poovuttikul, JHEP **02**, 085 (2018) doi:10.1007/JHEP02(2018)085 [arXiv:1708.08306 [hep-th]].
35 A. Amoretti, D. Aren, B. Goutraux and D. Musso, Phys. Rev. Lett. **120**, no.17, 171603 (2018) doi:10.1103/PhysRevLett.120.171603 [arXiv:1712.07994 [hep-th]].
36 W. J. Li and J. P. Wu, Eur. Phys. J. C **79**, no.3, 243 (2019) doi:10.1140/epjc/s10052-019-6761-0 [arXiv:1808.03142 [hep-th]].
37 M. Baggioli, Phys. Rev. Res. **2**, no.2, 022022 (2020) doi:10.1103/PhysRevResearch.2.022022 [arXiv:2001.06228 [hep-th]].
38 Y. Ling, P. Liu, J. P. Wu and Z. Zhou, Phys. Lett. B **766**, 41 (2017) doi:10.1016/j.physletb.2016.12.051 [arXiv:1606.07866 [hep-th]].
39 T. Andrade and A. Krikun, JHEP **05**, 039 (2016) doi:10.1007/JHEP05(2016)039 [arXiv:1512.02465 [hep-th]].